

Article

# Wave Energy Generation in Brazil: A Georeferenced Oscillating Water Column Inventory

Adriano Silva Bastos <sup>1,\*</sup>, Tâmara Rita Costa de Souza <sup>2</sup>, Dieimys Santos Ribeiro <sup>3</sup>,  
Mirian de Lourdes Noronha Motta Melo <sup>1</sup> and Carlos Barreira Martinez <sup>1,2</sup>

<sup>1</sup> Mechanical Engineering Postgraduate Program, Universidade Federal de Itajubá, Itajubá 37500-903, Brazil

<sup>2</sup> Graduate Program in Mechanical Engineering, Universidade Federal de Minas Gerais, Belo Horizonte 31270-901, Brazil

<sup>3</sup> Electrical Engineering Postgraduate Program, Universidade Federal de Itajubá, Itajubá 37500-903, Brazil

\* Correspondence: [adriano.bastos@unifei.edu.br](mailto:adriano.bastos@unifei.edu.br)

**Abstract:** Seas and oceans offer great potential as a widely available source of clean and renewable energy near high energy consumption centers. This source of energy is a valuable option in the energy transition and in energy matrix decarbonization. Wave energy and an oscillating water column (OWC) device stand out as the types of ocean energy with the most potential. An onshore OWC requires locations with rocky outcrops and steeper slopes as the device needs to be physically installed and has lower energy dissipation due to friction with the seabed. However, Brazil has approximately 7490 km of coastlines, with various shoreline geometries and geomorphologies, some of which are very suitable for OWC implementation. Some authors have estimated that the Brazilian coast has a total potential of 114 GW, distributed between wave and tidal energy, with a great possibility of contributing to global decarbonization efforts. This study aimed to identify and quantify the potential of locations suitable for implementing wave energy farms equipped with onshore OWC. For this, a prospect was carried out using the georeferencing software QGIS, resulting in a georeferenced map with a dataset of 319 locations, and determining a power capacity of exploitation of 9.84 GW and an estimated energy of 83,689 GWh/year in ten of the seventeen coastal states. This energy corresponds to twice the energy consumption of the state of Rio de Janeiro, which has a population of approximately 17.5 million people. If the same amount of wave energy as gas-fired thermal generation energy were to be consumed, the use of wave energy would reduce emissions by approximately 44.52 million tons of CO<sub>2</sub> annually. This result suggests that wave energy generation should be included in future studies on the expansion of Brazilian electric systems as an accelerating factor in the energy transition.

**Keywords:** energy resources; energy transition; ocean energy; oscillating water column; renewable energy; wave energy



**Citation:** Bastos, A.S.; Souza, T.R.C.d.; Ribeiro, D.S.; Melo, M.d.L.N.M.; Martinez, C.B. Wave Energy Generation in Brazil: A Georeferenced Oscillating Water Column Inventory. *Energies* **2023**, *16*, 3409. <https://doi.org/10.3390/en16083409>

Academic Editor: Frede Blaabjerg

Received: 22 March 2023

Revised: 7 April 2023

Accepted: 11 April 2023

Published: 13 April 2023



**Copyright:** © 2023 by the authors. Licensee MDPI, Basel, Switzerland. This article is an open access article distributed under the terms and conditions of the Creative Commons Attribution (CC BY) license (<https://creativecommons.org/licenses/by/4.0/>).

## 1. Introduction

Universal access to clean and renewable electricity is one of the seventeen sustainable development goals of the United Nations Development Program (UNDP) [1]. To achieve this goal, it is necessary to decarbonize the electricity generation process by promoting an energy transition from carbon-based to renewable and clean sources. According to Smil (2010) [2], past and future shifts in the energy base are inherent processes of human evolution and are carried out through changes in technology, economy, and society. The modern transition model proposes changes in the economy through technology, with society's commitment to transform the current energy base into one with lower carbon consumption, ensuring the conscious and sustainable use of natural resources.

Brazil's energy matrix, with an installed capacity of 174.7 GW (2020), mainly consists of renewable energy sources (84%) [3]. The current matrix includes 62.5% from hydroelectric

power plants (from large to small power plants); 21.5% from other renewable sources, such as biomass, solar, and wind; and 16% from nuclear and carbon-based sources, such as oil, coal, and natural gas [3]. Brazil ranks 12th among the countries with the highest CO<sub>2</sub> emissions in the world, with 441 million tons of CO<sub>2</sub>eq, according to data from the Emissions Database for Global Atmospheric Research (EDGAR) from the European Commission [4]. Brazil ratified the Paris Agreement [5] in 2015, committing to a Nationally Determined Contribution (NDC) goal of reducing its greenhouse gas (GHG) emissions by 37% by 2025 and by 43% by 2030, compared with its levels in 2005. In 2021, Brazil further pledged to achieve a 50% reduction in GHG emissions by 2030 and to reach carbon neutrality by 2050 [6].

In Brazil, the National Energy Plan (PNE) report [7,8] outlines the energy planning strategies and goals for the next 30 years. The most recent document [8] considers the expansion of the energy matrix from the perspectives of the energy transition and energy matrix decarbonization. Two hypotheses are presented: the first involves increasing the use of renewable energy by 100% and not increasing the use of fossil fuel sources. In contrast, the second involves increasing the use of fossil fuel sources if carbon sequestration occurs, resulting in a 0% emission expansion. In this PNE [8], two extreme economic scenarios were established for Brazil: a pessimistic scenario, characterized by stagnant economic growth but maintenance of the current electricity demand, and an optimistic scenario, characterized by accelerated economic growth that requires a 330% increase in the electricity supply from the levels in 2020. If the economy stagnates, the energy matrix will naturally expand. However, if the economy experiences much growth, the energy matrix needs to expand quickly, presenting challenges in ensuring steady supply as consumption is forecasted to increase from 621 TWh/year, recorded in 2020 [3], to 2053 TWh/year in 2050 [8]. In the high economic growth scenario, the report encourages the use of photovoltaic and wind energy, which are renewable, clean, and non-carbon-emitting sources. However, the report also considers the possible implementation of carbon-based thermal projects and new large hydropower plant projects, including, if necessary, Amazonian plants with environmental restrictions, which may contradict the decarbonization, energy transition, and GHG emission reduction goals [8].

Ocean energy only appears in expansion plans as part of the matrix of available energy resources [8]. Even when ocean energy is specifically addressed, only the international panorama and its national theoretical potential are highlighted, emphasizing the need for studies on tidal currents energy and pointing out ocean thermal energy as a promising resource in Brazil. However, when considering the geomorphological characteristics of the Brazilian coast, it becomes apparent that there is a coastal strip of approximately 7490 km, which includes various geometries and morphologies for the shorelines, some of which are potentially suitable for the implementation of wave energy farms. Overall, a theoretical potential of the order of 114 GW (998 TWh/year) was estimated for the Brazilian coast, which was subdivided into 27 GW of tidal potential and 87 GW of wave potential [9], a value that corresponds to 1.6 times the Brazilian energy consumption in 2020 (621 TWh/year [3]). Despite this potential, in Brazil, there are only experimental projects using this type of energy, with the most relevant being the tidal project of the Bacanga dam [10] and the wave pilot project of the Pecém port [11]. The latest one, designed by the Alberto Luiz Coimbra Institute of Graduate Studies and Research in Engineering (COPPE) of the Federal University of Rio de Janeiro (UFRJ) in partnership with Tractebel-Engie S.A., had a capacity of 50 kW and was implemented in 2012 on the port's breakwater. The project aimed to test a wave energy harvesting technology where large floats coupled to articulated mechanical arms pressurized freshwater into accumulators connected to hyperbaric chambers. The internal pressure of these chambers corresponded to 200 and 400 m in the water column and activated a Pelton turbine [11]. Despite the positive results, this project was discontinued and is currently inactive (2022) [12]. Despite the experiments developed in Brazil, there are still no legal devices or any specific legislation regarding the implementation of ocean energy parks. This is due to the fact that the country still has a

reasonable amount of available hydraulic potential and has made advances in wind and solar energy, which have competitive costs.

The United States, China, and the United Kingdom, as well as other European countries, have been discussing and encouraging research and development of ocean energy as an alternative to diversify their energy matrix [13,14]. Since the oil crisis in 1973, these countries have been seeking alternative ways to ensure their energy security without depending on oil [13]. The pioneering work in modern studies on the use of ocean energy was carried out in Japan in 1940 by Yoshio Masuda, who developed a signaling buoy fitted with a turbine driven by wave motion. Masuda also built a barge equipped with converters of various configurations and turbines, thus expanding the research on wave energy conversion [15]. Since then, numerous researchers have dedicated themselves to studying wave energy over the past five decades (1970–2020). Salter [16] published a study on wave energy in 1974 that attracted global attention to this energy resource. McCormick [17] became the first academic author to publish a book dedicated to this topic, in 1981 [14]. Evans [18,19] and Falnes [14,20] focused on studying wave–device interactions. Falcão [13], in Portugal, studied oscillating water column (OWC) devices [21,22] and their interaction with self-rectifying turbines [23–25]. Setoguchi [26,27] and Raghunathan [28,29] worked on designing and optimizing Wells-type self-rectifying turbines. Ocean energy harvesting technology is still developing and maturing despite these efforts over the past fifty years. Although it presents potential as a significant energy resource, using this energy still involves high costs in both the implementation and production phases [30], posing a challenge to the technology's commercial viability.

This study aimed to identify and quantify the energy potential from ocean waves in Brazil by harvesting energy from an onshore oscillating water column (OWC) device and an onshore standardized OWC micro-module (OWCMM) device. For this, the wave climate for the entire Brazilian coast was characterized, obtaining significant wave height ( $H_s$ ) and peak wave period ( $T_e$ ) values, which were used to determine the energy flux ( $E_f$ ) for each coastal state. A georeferenced survey of the entire coast was conducted to identify locations that meet the requirements of a promontory area and a slope above 0.01 m/m, which are necessary to determine the feasibility of implementing electricity-generating farms. The exploitable potential and available energy were calculated for each region where the area yielded a positive result regarding the implementation of generating farms. This study also provides a shapefile map containing the energy results dataset with the geographic coordinates of each location. Additionally, the amount of GHG emissions that could be reduced by using this energy source compared with using traditional sources could contribute to decarbonizing the energy matrix was estimated.

### 1.1. Ocean Energy

There are five methods for harnessing ocean energy, each with a specific converter device and a distinct exploitation area, whether onshore, nearshore, or offshore [12,31]. Salinity gradient energy is obtained through the difference in salinity concentration between seawater and freshwater or simply through the salinity concentration difference in seawater [32]. So far, only two techniques are viable for extracting this energy: Reverse Electrodialysis (RED), which extracts energy directly from the chemical process, and Pressure Retarded Osmosis (PRO), which uses the pressure difference resulting from osmosis [33]. Ocean thermal gradient energy is obtained through the temperature difference in seawater, which requires a minimum difference of 20 °C, which is only possible below an 800 m depth. The process of conversion into electrical energy uses the Rankine cycle, transforming thermal energy into mechanical energy [34]. In harnessing tidal current energy, the hydrokinetic energy due to the upward and downward movements of the astronomical tide is harvested, which drives a turbine generator group. This harnessed energy resembles wind and hydraulic energy [35]. Tidal range energy is the most consolidated form of ocean energy and has been used in commercial applications since the 1960s (La Rance tidal barrage, in 1966, 240 MW [36]). Its energy potential is due to the upward and downward

movements of the astronomical tide, and its operating principle is similar to a hydropower plant. During upward movement of the tide, water is stored in a barrage, and when the tide recedes, the amount of flow decreases and the stored water is then used to generate electricity through a turbine [37,38].

Wave energy is the form of ocean energy with the highest energy density, being up to 30 times more concentrated than solar energy [9,14]. The wave generation process combines wind and solar energy into kinetic and potential energy, transporting it from one location to another. The heating of the atmosphere, resulting from solar radiation, creates an imbalance in pressure between the layers of air masses, causing them to move. This movement creates a thrust and suction channel, giving rise to winds. When these winds reach the ocean surface, they cause shear stress, resulting in surface deformation of the water: the stronger and more continuous the wind, the greater the deformation amplitude. Once generated, waves can travel long distances without significant energy losses. In a wave, kinetic energy is derived from the horizontal movement of the water mass, and potential energy originates from the circular orbital motion of the water particles in the displaced mass [31,37]. Wave energy is the one that arouses the greatest scientific interest among the five forms of ocean energy, whether due to its apparent form (wave motion) or its magnitude scale (tsunamis). However, this energy also has the disadvantage of being inconsistent; waves, similar to the winds that generate them, have significant variability and randomness, which can vary consecutively from one wave to another [13]. This fact directly affects the energy production efficiency. As a relatively new, disruptive, and emerging form of energy exploitation, wave energy requires more studies, research, and development to improve the performance of its converter devices and to adjust its implementation, and operation and maintenance costs for commercial viability [30,39]. Among the technologies and devices developed for harvesting wave energy into electricity are overtopping devices [40,41], submerged pressure differential devices [42], attenuator devices [43,44], point absorber devices [45], rotation mass devices [42], oscillating body devices [46], and oscillating water column devices [13,15].

Although tidal energy conversion technology is the most consolidated among ocean energies, benefiting from the maturity of classical hydraulic generation, wave energy has greater applicability due to the variety of converter devices and exploration fields: onshore, nearshore, and offshore. According to Lin et al. (2015) [47], installing a converter device on the coastline is advantageous in operation and maintenance, being easily accessible and keeping the generator group away from the water. Onshore installations also lead to easy connection to the electrical grid, eliminating the need for submarine cables. Therefore, based on these facts and an exploration of the coastlines near Brazil's major energy consumption centers, this study was limited to an analysis of the wave energy on the coastline.

## 1.2. Ocean Energies Resources

According to 2020 data from the International Renewable Energy Agency (IRENA) (2020) [48,49], global theoretical potential estimates for ocean energy harnessing are on the order of 76,350 TWh/year, excluding tidal range energy. When the global assessment for tidal range energy, which according to Neill et al. (2018) [36] is 25,880 TWh/year, is included, the total estimated potential increases to 102,230 TWh/year (Figure 1b). In terms of local potential, a 2013 study conducted by COPPE in collaboration with Seahorse Wave Energy (SWE) [9] estimated the ocean potential of the Brazilian coast to be approximately 114 GW, divided between tidal range and wave energy (Figure 1a). The COPPE/SWE study detailed the potential for each coastal state of Brazil, the values of which are presented in Table 1.

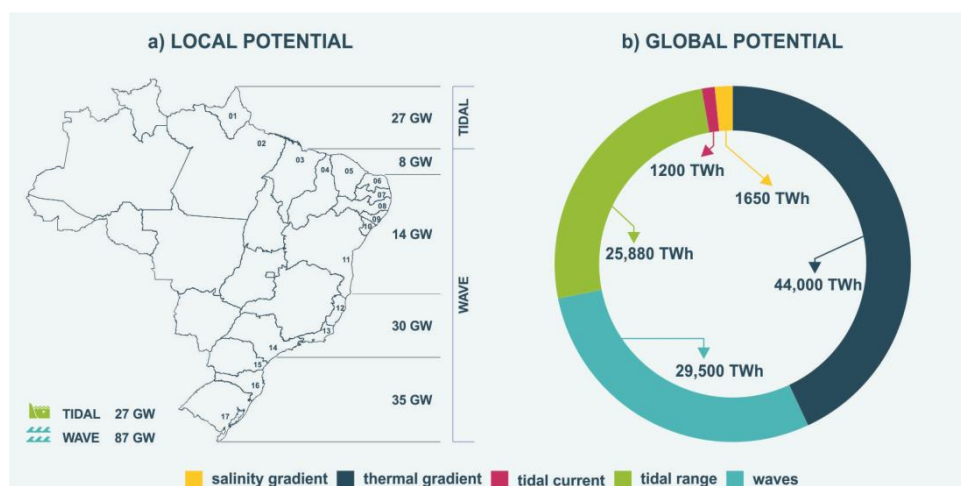


Figure 1. Global and local potential. Source: [9], adapted from [36,48].

Table 1. Estimated potential of the Brazilian coast. Source: [9].

Coastal State	Potential (GW)	Coastal State	Potential (GW)		
01	Amapá	7.81	10	Sergipe	2.47
02	Pará	7.30	11	Bahia	14.10
03	Maranhão	8.35	12	Espírito Santo	5.94
04	Piauí	0.96	13	Rio de Janeiro	9.80
05	Ceará	8.38	14	São Paulo	9.60
06	Rio Grande do Norte	6.00	15	Paraná	1.51
07	Paraíba	1.84	16	Santa Catarina	10.90
08	Pernambuco	2.94	17	Rio Grande do Sul	12.80
09	Alagoas	3.60		Brazil	114.30

In 2020, Ocean Energy Systems (OES) (2020) [50] reported that the installed and operational ocean energy capacity worldwide was 534.69 MW, distributed as follows: (i) tidal range (barrage), 521.50 MW; (ii) tidal current, 10.60 MW; (iii) wave, 2.31 MW; (iv) ocean thermal gradient, 0.23 MW; and (v) salinity gradient, 0.05 MW. Furthermore, the International Renewable Energy Agency (IRENA) (2020) [48] predicts that an additional 1907 MW of tidal current energy and 149.7 MW of wave energy will be added in the short term, resulting in a total capacity of 2591.36 MW by 2025, and estimates a total installed power of 10 GW by 2030.

### 1.3. Oscillating Water Column Device

Studied since 1940, the oscillating water column (OWC) device is one of the most suitable ocean energy conversion devices, having even achieved commercial status. These devices have an arrangement inspired by natural resonant cavities that form in rocky slopes and expel seawater as a geyser (blowholes). It comprises primarily a hydropneumatic chamber filled with air, in which an opening facing the ocean allows the lifting and lowering action of the wave to exert a pressurizing and depressurizing force on the chamber, forcing the displaced air to drive a turbine at the device outlet [13,51]. According to Rosati et al. (2022) [52], oscillating water column (OWC) devices have advantages over other converter devices. In a typical OWC, the moving parts are limited to the turbine-generator group, and this electromechanical set is located above the water surface, improving device reliability and simplifying maintenance. According to Ilyas et al. (2014) [53] and Contestabile et al. (2020) [40], these devices can have positive effects on reducing coastal erosion. However, other authors mentioned in their studies that there are negative effects that should be further investigated in order to have a more accurate overview of environmental impacts [44]. The shoreline installation of the converter is considered a positive point, as

it allows for easy access during construction, operation, and maintenance, as well as easy connection to the power grid, dispensing maritime electrical wiring installation, which directly reduces the costs involved [13,30]. Some authors mentioned that, regarding clean and renewable energy, the use of OWC technology has almost no impact on the environment [21,54], with some of the significant environmental impacts observed being the noise emitted by the turbine, the visual impact on the landscape, and bird and fish collisions with the structure. However, using OWC technology for electricity generation does not emit GHG, and around 4660 tons of CO<sub>2</sub> equivalent per MW can be decarbonized in one year [55].

According to Falcão apud Zhang (2021) [56], the whole process of wave energy conversion consists of three stages. In the case of an OWC device, the first stage consists of absorbing the hydrodynamic energy of the wave (kinetic and potential) in the form of pneumatic compression of a volume of air. The second stage consists of the power take-off (PTO), harnessing the useful mechanical energy from the air displacement in the chamber and converting it into torque energy in the turbine. The third stage involves the generator converting this mechanical energy into electricity. Falcão and Henriques (2016) [15] explored, in their work, the main characteristics and evolution of OWC devices. The authors emphasized that the best turbine option for equipping this converter is a self-rectifying axial turbine, such as the Wells turbine and the action turbine, which maintain the direction of rotation independently of the direction of air flow (bidirectional). As mentioned in Section 1.1, the disadvantage of wave energy is its variability and randomness, which leads to greater complexity in designing a PTO, as the turbine is subject to oscillations in air pressure and flow rate. However, what matters in terms of aerodynamic performance is the average efficiency and not the maximum efficiency [15]. Raghunathan and Tan (1982) (1983) [29,57] studied the performance of the Wells turbine, which is a reversible low-pressure axial flow turbine. Its blades have a symmetrical airfoil in relation to its rotation plane and perpendicular to the air flow. The tangential force of the air flow acts on the blade, exerting a rotational torque independent of the direction of flow. Its efficiency is lower than that of an axial turbine with asymmetric blades because it has a higher drag coefficient than the asymmetric ones, even when working under ideal conditions [29,57]. Regarding the electric generator, Falcão et al. (2020) [21] stated that it is possible to use a standard synchronous generator. However, a more complex control system is required due to the variability and randomness of the waves. The safest choice to equip an OWC is a variable speed generator, which responds more efficiently to this range of variations. A Doubly Fed Induction Generator (DFIG) has been a popular choice for variable rotational speed wind energy conversion systems interfacing with the electrical grid and is perfectly applicable to an OWC.

The greatest challenge facing this technology is its currently high implementation cost. It is estimated to range from USD 2700 to 9100 per installed kW [8]. According to Callaghan (2006) [30], who analyzed the costs and competitiveness of wave and tidal current energies, the cost of a wave energy prototype can range from 7869 USD/kW to 16,470 USD/kW. In Andres et al. (2017) [39], the authors assumed a linearized cost of energy (LCOE) of 0.18 USD/kWh and arrived at an average implementation cost of 3241 USD/kW. Edenhofer et al. (2012) [54] presented a chart of the implementation evolution cost per kilowatt (USD/kW) and predicted an 11% reduction with every doubling of installed capacity. It is estimated that, by 2030, the cost will reach values between USD 4000 and 6000 per installed kW, which is like the implementation cost of a small hydroelectric plant [8].

Successful prototypes and pilot projects of OWC have been developed worldwide. These devices are pioneers and considered first-generation, and their experiences have led to technological advances in new projects [58,59]. In recent years, several advancements have been made in OWC technology, including using advanced materials and incorporating new designs and control systems. These advancements have increased the efficiency and reliability of the device, making it more attractive for commercial use [13].

## 2. Materials and Methods

To achieve the goals of identifying and quantifying the exploitable potential of wave energy through oscillating water column (OWC) devices, this study began with identifying the wave climate along the Brazilian coast to obtain the significant wave height ( $H_s$ ) and peak period ( $T_e$ ) parameters. These data are essential for calculating the energy flux ( $E_f$ ), which provides the amount of energy available in a wave expressed as power per unit length [W/m]. The energy flux was then used to calculate the maximum available power, whether for an area of interest for exploitation or a converter device. To do this, one multiplies the linear length or width of the device by the energy flux, thus obtaining the power [W], and consequently, it is possible to calculate the maximum available energy [Wh]. To identify suitable locations for wave energy exploitation, a georeferenced survey was conducted using QGIS software. This survey was undertaken kilometer by kilometer, verifying whether the area in focus has a rocky slope or sandy beach. In the case of a rocky slope, the distance between the coastline and the  $-20$  m bathymetric line was verified to ensure a slope greater than  $0.01$  m/m. At the end of the survey, a georeferenced map was prepared to note the geographic coordinates of the acquired points and the length vector of each area. Figure 2 schematically describes the activity flow method employed in this study.

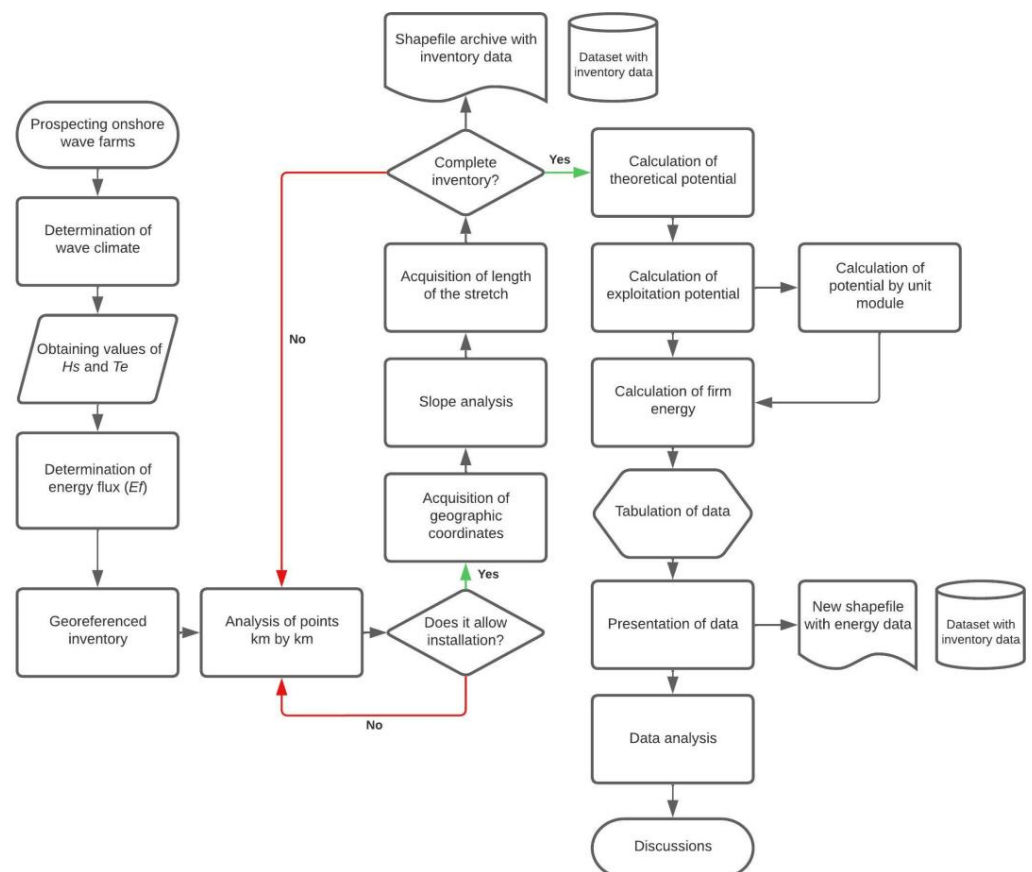


**Figure 2.** Methodology flowchart.

### 2.1. Wave Climate

Wave climate involves a statistical analysis of a set of wave data over a specific period of time [60]. From this analysis, important parameters such as significant wave height ( $H_s$ ), peak wave period ( $T_e$ ), and wave direction ( $D_s$ ) can be obtained and were used to determine the probability distribution of the wave behavior. Significant wave height ( $H_s$ ) is a statistical parameter representing the average of the highest one-third ( $1/3$ ) of the analyzed samples. It is important to note that  $H_s$  differs from individual wave height ( $H$ ). The peak wave

period ( $T_e$ ) is the time required for a wave to travel a certain length from crest to crest [61]. These parameters are fundamental for determining the energy flux ( $E_f$ ) transmitted by the wave. Pianca et al. (2010) [62] conducted a reanalysis of the Brazilian wave climate using 11 years of data (1997 to 2007) obtained from the WaveWatch III wave model [63]. The authors subdivided the coastline into six sectors along the Brazilian continental shelf break. They concluded that there is an increase in energy levels from north to south along the entire Brazilian coast. It became evident that, in sectors W1 to W4 (from the extreme south of Rio Grande do Sul to the north of Alagoas), waves are more energetic in winter, while in sectors W5 and W6 (from the north of Alagoas to Amapá), waves are more energetic in summer (December to March in South America). Carvalho (2010) [64] also conducted a study on the wave climate of the Brazilian coast, using a series of 12 years of data (1997 to 2009) from the WaveWatch III model [63]. The study was divided into ten areas of similarities related to wave systems. The author characterized the wave climate by determining significant heights and peak wave periods, as well as monthly and annual averages of wave energy. Espindola (2017) [65] conducted a reanalysis of the wave climate, using 35 years of data (1979 to 2014) obtained from the ERA-Interim project [66] as input for the model. The author used 49 points along the entire Brazilian coast (Figure 3) to determine significant wave heights and peak wave periods for the 50% ( $H_s P_{50}$ ), 95% ( $H_s P_{95}$ ), and maximum ( $H_s max$ ) percentiles, which are presented in Table 2.

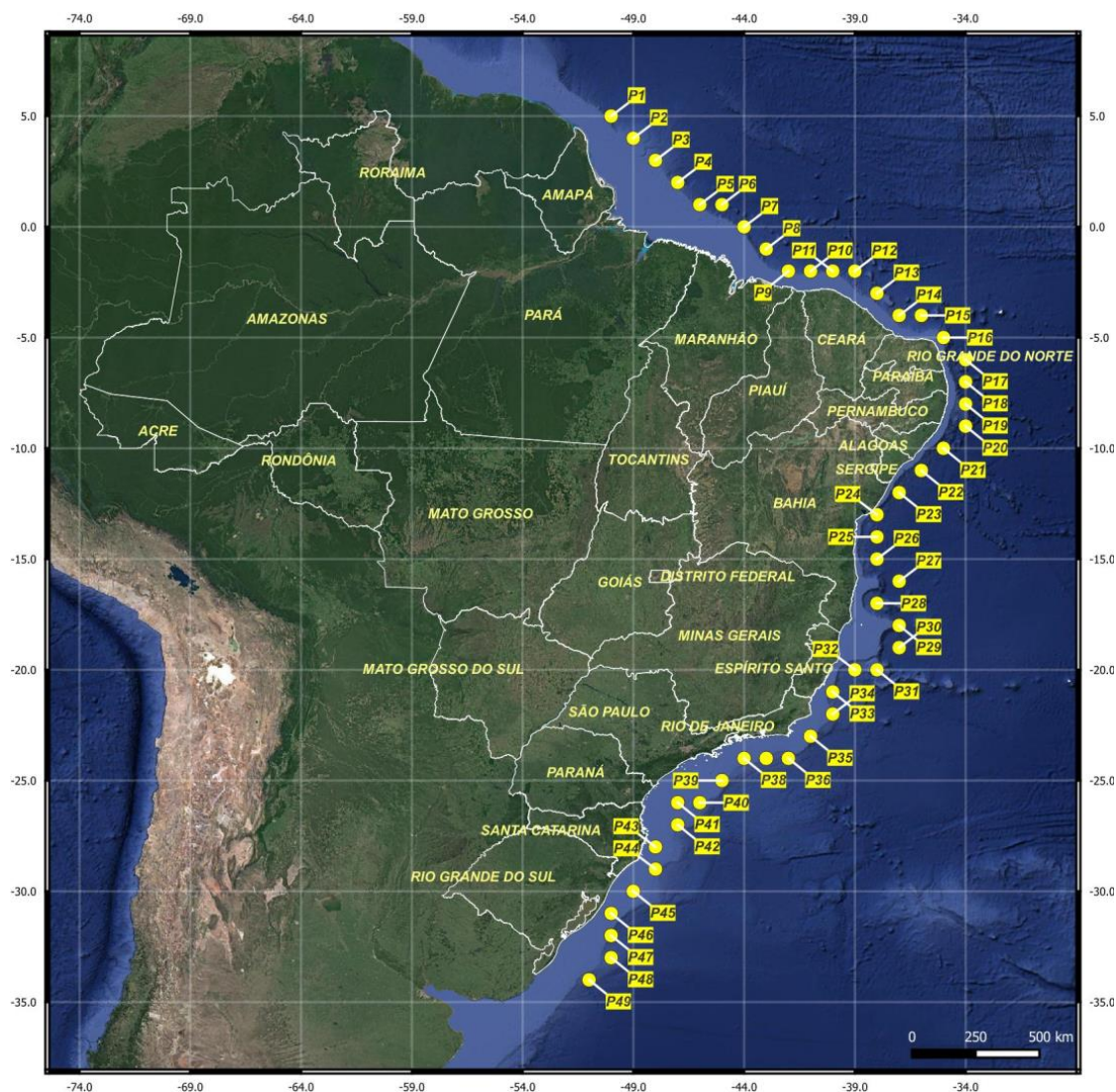


Figure 3. List of study points on wave climate. Adapted from [65].

**Table 2.** Significant wave heights and peak wave periods. Adapted from: [65].

Point	Lat	Lon	Coastal State	$H_S P_{50}$ (m)	$H_S P_{95}$ (m)	$H_{S MAX}$ (m)	$\overline{H_S P_{50}}$ (m)	$T_e$ (s)	$\overline{H_S P_{95}}$ (m)	$T_e$ (s)	$\overline{H_{S MAX}}$ (m)	$T_e$ (s)
P 01	5.00	−50.00		1.66	2.41	3.68						
P 02	4.00	−49.00	Amapá	1.64	2.35	3.59	1.64	8.00	2.34	8.50	3.57	12.00
P 03	3.00	−48.00		1.62	2.27	3.45						
P 04	2.00	−47.00	Pará	1.60	2.18	3.36	1.59	8.00	2.14	8.50	3.30	12.00
P 05	1.00	−46.00		1.58	2.09	3.23						
P 06	1.00	−45.00		1.64	2.17	3.48						
P 07	0.00	−44.00	Maranhão	1.62	2.13	3.25	1.64	7.50	2.16	8.50	3.19	12.50
P 08	−1.00	−43.00		1.65	2.18	3.08						
P 09	−2.00	−42.00		1.63	2.17	2.95						
P 10	−2.00	−41.00	Piauí	1.67	2.18	3.02	1.67	7.50	2.18	8.00	3.02	12.50
P 11	−2.00	−40.00		1.67	2.17	2.96						
P 12	−2.00	−39.00	Ceará	1.72	2.25	3.08	1.68	7.50	2.19	8.00	3.02	12.50
P 13	−3.00	−38.00		1.70	2.21	2.99						
P 14	−4.00	−37.00		1.64	2.12	3.04						
P 15	−4.00	−36.00		1.72	2.22	3.14						
P 16	−5.00	−35.00	Rio Grande do Norte	1.63	2.06	2.91	1.72	7.50	2.20	8.00	3.22	11.00
P 17	−6.00	−34.00		1.81	2.32	3.61						
P 18	−7.00	−34.00	Paraíba	1.77	2.28	3.69	1.77	8.00	2.28	8.00	3.69	9.50
P 19	−8.00	−34.00		1.73	2.28	3.72						
P 20	−9.00	−34.00	Pernambuco	1.76	2.36	3.77	1.75	8.00	2.32	8.50	3.75	10.50
P 21	−10.00	−35.00		1.62	2.26	3.52	1.62	8.00	2.26	8.50	3.52	11.50
P 22	−11.00	−36.00	Alagoas Sergipe	1.55	2.21	3.63	1.55	8.00	2.21	8.00	3.63	10.00
P 23	−12.00	−37.00		1.54	2.22	4.02						
P 24	−13.00	−38.00		1.42	2.11	3.98						
P 25	−14.00	−38.00		1.44	2.14	4.12						
P 26	−15.00	−38.00	Bahia	1.43	2.11	3.93	1.51	8.00	2.20	8.00	4.05	8.50
P 27	−16.00	−37.00		1.60	2.31	4.17						
P 28	−17.00	−38.00		1.46	2.10	3.62						
P 29	−18.00	−37.00		1.67	2.42	4.51						
P 30	−19.00	−37.00		1.73	2.52	4.85						
P 31	−20.00	−38.00	Espirito Santo	1.73	2.55	4.52	1.64	8.50	2.40	9.00	4.31	10.00
P 32	−20.00	−39.00		1.63	2.39	4.30						
P 33	−21.00	−40.00		1.48	2.13	3.58						
P 34	−22.00	−40.00		1.74	2.54	4.42						
P 35	−23.00	−41.00	Rio de Janeiro	1.79	2.64	5.07	1.79	9.00	2.68	9.50	5.23	11.50
P 36	−24.00	−42.00		1.87	2.82	5.81						
P 37	−24.00	−43.00		1.76	2.71	5.60						
P 38	−24.00	−44.00		1.64	2.57	5.16						
P 39	−25.00	−45.00	São Paulo	1.72	2.72	5.56	1.70	9.50	2.69	9.50	5.48	11.00
P 40	−26.00	−46.00		1.73	2.77	5.71						
P 41	−26.00	−47.00	Paraná	1.55	2.47	4.85	1.55	9.00	2.47	9.00	4.85	10.50
P 42	−27.00	−47.00		1.71	2.76	6.45						
P 43	−28.00	−48.00	Santa Catarina	1.77	2.83	6.78	1.78	9.00	2.86	9.00	6.97	10.50
P 44	−29.00	−48.00		1.86	3.00	7.68						
P 45	−30.00	−49.00		1.80	2.90	6.44						
P 46	−31.00	−50.00		1.84	3.03	6.59						
P 47	−32.00	−50.00	Rio Grande do Sul	1.97	3.30	7.18	1.95	9.00	3.28	9.00	7.01	10.50
P 48	−33.00	−50.00		2.10	3.59	7.46						
P 49	−34.00	−51.00		2.06	3.57	7.37						

The meanings of the symbols are as follows:  $H_S$ —significant wave height;  $T_e$ —peak wave period;  $P_{50}$ —50% percentile;  $P_{95}$ —95% percentile;  $P_{max}$ —maximum height.

## 2.2. Wave Energy Potential Estimation

Wave energy comprises the sum of the potential energy ( $PE$ ) and kinetic energy ( $KE$ ). Both are obtained as a function of the individual wave height ( $H$ ), the density of seawater ( $\rho$ ), and the acceleration of gravity ( $g$ ), expressed by Equations (1) and (2) below. It is a conservative system (Equation (3)) expressed in ( $N/m^2$ ) [37,61].

$$PE = \frac{1}{16} \cdot \rho \cdot g \cdot H^2 \quad (1)$$

$$KE = \frac{1}{16} \cdot \rho \cdot g \cdot H^2 \quad (2)$$

$$E = PE + KE = \frac{1}{8} \cdot \rho \cdot g \cdot H^2 \quad (3)$$

When determining the energy flux ( $Ef$ ), which represents the amount of energy available per meter of wave front [W/m], it is necessary to multiply the total energy ( $E$ ) (Equation (3)) by the group velocity ( $Cg$ ) [m/s], where  $Cg = nC$ , with  $n$  being the wave celerity factor (dimensionless) and  $C$  being the wave celerity (m/s). According to Dean and Dalrymple (1991) [61], the energy flux ( $Ef$ ) is given by Equation (4).

$$Ef = E \cdot n \cdot C = \left( \frac{1}{8} \cdot \rho \cdot g \cdot H^2 \right) \cdot n \cdot \left( 1 + \frac{2 \cdot k \cdot h}{\sinh(2 \cdot k \cdot h)} \right) \cdot \frac{\omega}{k} \quad (4)$$

where  $k$  is the wave number given by ( $k = 2\pi/L$ ),  $L$  is the wavelength from crest to crest (m),  $\omega$  is the angular frequency given by ( $\omega = 2\pi/T$ ) (Hz),  $T$  is the wave period (s), and  $h$  is the local depth (m).

According to Dean and Dalrymple (1991) [61], the factor  $n$  assumes values of 1/2 for deep water and 1 for shallow water. This factor's value means that, in deep water, energy is transmitted at half the speed of the waves, while in shallow water, the energy flow follows the same speed as the waves. The real state of the sea is described as the sum of a large number of regular waves with different frequencies, amplitudes, and directions, better described by the spectral variation in the density function or 2D wave spectrum [67,68]. For the analysis of energy flux in a spectrum, the total energy ( $E$ ) per unit area is considered as the integral of the total energy as a function of the wave spectrum (Equation (5)) [60,64]. With  $Ef$  established for deep waters at the spectral analysis point, Equation (5) can be simplified into Equation (6). The mathematical development is shown in Folley (2017) [69].

$$Ef = \int_0^{\infty} \rho \cdot g \cdot E \cdot (\omega) \cdot \frac{1}{2} \cdot \frac{\omega}{k(\omega)} \left( 1 + \frac{2 \cdot k \cdot (\omega) \cdot h}{\sinh(2 \cdot k \cdot (\omega) \cdot h)} \right) d\omega \quad (5)$$

$$Ef = \frac{\rho \cdot g^2}{64\pi} \cdot H_S^2 \cdot T_e \quad (6)$$

The energy system contained in the wave spectrum, or a solitary wave, is conservative, meaning that its energy flux ( $Ef$ ) is conserved along the wave propagation path. However, when propagating towards the coast, there is a change in wave velocity and height due to shoaling and refraction, compensating the system and keeping it conserved. However, there is an energy dissipation through friction with the seabed. According to Ostritz (2012) [70], there is an energy loss between 5 and 10% when the waves approach the coastline. As this study considers the location of the converter devices installed on promontories with steep slopes, a loss of 5% due to friction from the spectral analysis point to the coast was considered. The amount of energy calculated in this work, the average significant wave height of the 95th percentile ( $\overline{H_S P_{95}}$ ), and their respective peak wave periods ( $T_e$ ) presented in Table 2 were considered, along with the energy value obtained through Equation (6).

### 2.3. Wave Energy Converter

Wave climate, geometric design of the capture chamber, and turbine efficiency determine the overall performance of an oscillating water column (OWC) device. The most widely accepted option for equipping OWC devices is the self-rectifying reversible flow turbines [15,46], which include the Wells turbine and its variants [71], the guide vane action turbine, and the bi-radial turbine [72]. The Wells turbine is an axial flow generator that uses symmetric airfoil blades arranged radially at 90°. The tangential force produced by the flow on the rotor blades depends only on the angle of incidence of the relative flow, regardless of the flow direction [15]. Falcão et al. (2018) [73] compared different self-rectifying turbine models to determine their efficiency and found efficiency rates ranging from 53.8% to 63.7% ( $\bar{\eta} = 59.04\%$ ) for Wells turbines with one plane and no guide vanes (dependent on rotor solidity and the number of blades), from 62.5% to 70.1% ( $\bar{\eta} = 66.3\%$ ) for one-plane Wells tur-

bines with guide vanes, 53.35% for bi-plane turbines, and 60.9% for contra-rotating turbines. The authors also concluded that the Wells turbine with one plane and no guide vanes is the cheapest of the models presented. The guide vane action turbines can achieve efficiencies of up to 59.4%, and the bi-radial turbines can reach efficiencies of up to 72% [73]. Although these turbines have higher efficiencies, they are considerably more expensive than the Wells turbines, with one plane and no guide vanes [73] and will not consider in this study. The Wells turbine defined for this study considers the optimizations of Raghunathan and Tan (1983) [29], who obtained better aerodynamic performance for a solidity coefficient, at 0.6. This coefficient represents the measure of flow blockage by the turbine and interference of the blades. An increased solidity value negatively influences the turbine performance, increasing the losses in kinetic energy that passes through the turbine. The authors also achieved better performance when the ratio between the hub diameter and the outer diameter of the turbine was 0.6, as smaller values can cause premature turbine stalling and decrease aerodynamic efficiency. In Raghunathan et al. (1985) [74], the authors concluded that the ideal number of blades should always be between four and six. Regarding the rotor blades, Mohamed et al. (2011) [75] studied symmetrical airfoil profiles NACA 0012, NACA 0015, NACA 0018, and NACA 0021, obtaining better efficiency for the latter. As for the electrical generator system, the use of a Doubly Fed Induction Generator (DFIG) with an adaptive speed control system is considered to maximize conversion efficiency by reducing turbine stalling [52,76].

Dizadji and Sajadian (2011) [77] stated that the overall efficiency of an OWC device depends on the individual efficiencies of the oscillating air column and the turbine. In their study on chamber geometry, the authors found an overall efficiency of 32% for the best geometry, with the chamber opening at an angle of 30° relative to the vertical plane. Ibarra-Berastegi et al. (2018) [78] analyzed the performance of the Mutriku wave power plant between 2014 and 2016 and found an overall conversion efficiency of 41%. Babarit (2015) [79] conducted a comparative study of the efficiency of wave energy converters and their capture width, presenting the overall efficiencies of various OWC devices. In his research, Babarit (2015) [79] reported overall efficiencies ranging from 7% to 20% for first-generation OWC devices and from 22% to 72% for third-generation OWC devices. Based on the data from this author, an overall average efficiency of approximately 44% for coastal OWC devices can be observed, and this value was used for the calculations in this study.

In addition to determining the potential for exploiting wave energy using onshore OWC devices, this study proposed calculating power and energy through standardized OWC micro-modules (OWCMM) capable of serving different regions of the Brazilian coast. The use of these micro-modules does not aim for maximum unit efficiency but for maximum utilization of the available potential, even at the expense of the system's overall efficiency. For this study, standardized power of each OWCMM was determined using Equation (7), which considers  $E_f$ ; the width of the module ( $L$ ) in meters (wave capture width), which was considered a standard of 6 m for all modules; and an efficiency ( $\eta$ ) of 44%, determined by Babarit (2015) [79].

$$P = E_f \cdot L \cdot \eta = \frac{\rho \cdot g^2}{64\pi} H_S^2 \cdot T_e \cdot L \cdot \eta \quad (7)$$

The first area covers the states of Amapá to Espírito Santo (P01 to P33), with an energy flux ranging from 15 to 20 kW/m, resulting in module power ranging from 40.06 kW to 54.85 kW. The second area, between the states of Rio de Janeiro and Santa Catarina (P34 to P44), has an energy flux ranging from 21 to 29 kW/m, resulting in modular power ranging from 57.85 kW to 77.74 kW. Finally, the area of the state of Rio Grande do Sul (P45 to P49) has an energy flux of 38 kW/m with a maximum power of 101.90 kW. The calculations resulted in power outputs of 55 kW for OWCMM1, 75 kW for OWCMM2, and 100 kW for OWCMM3.

The sizing of these micro-modules followed the premises proposed by Chen et al. (2021) [80] and Letzow et al. (2017) [81], and the quantities proposed by Lekube et al. (2018, 2015) [51,82], resulting in the calculated dimensions presented in Figure 4.

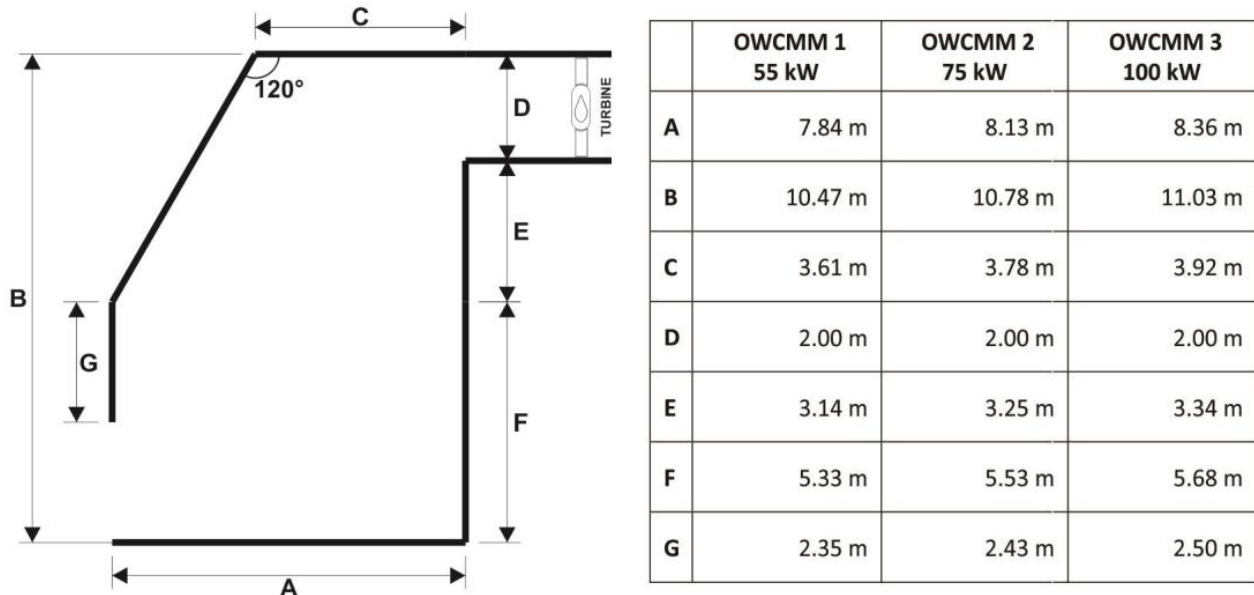


**Figure 4.** Basic dimensions of the adopted oscillating water column micro-modules.

The annual energy ( $E$ ) can be obtained using Equation (8), multiplying the power by time and the availability index ( $ai$ ), which represents the amount of generation time still available following installation.

$$E = P \cdot ai \cdot 8760 \text{ hours} \quad (8)$$

The generated energy cost ( $GEC$ ) is obtained as a function of the annual cost ( $AC$ ) of the installation added to its operation and maintenance cost ( $O\&M$ ) and divided by the annual energy ( $E$ ). The  $AC$  is calculated by multiplying the capital cost ( $Ccap$ ) by the capital recovery factor ( $CRF$ ), which is given by Equation (9).

$$CRF = \frac{(1+i)^n \cdot i}{(1+i)^n - 1} \quad (9)$$

where " $n$ " is the number of annuities received and " $i$ " is the interest rate.

According to Bosserelle et al. (p. 9) [83], the operation and maintenance ( $O\&M$ ) cost for a USD 270 million installation is USD 13.1 million, which represents an  $O\&M$  cost of 4.7% for this type of installation. De Andres (p. 90) [39] recommends using an interest rate of 12% per year. We adopted these values to calculate the payback of the installation. Equation (10) allows for the calculation of the  $GEC$  of the installation.

$$GEC = \frac{(Ccap \cdot CRF) + O\&M \text{ cost}}{E} \quad (10)$$

This study assumed that 1 kWh of thermal generation from a natural gas combined cycle power plant has an emission factor ( $EF$ ) of 532 gCO<sub>2</sub>eq/kWh, while for an oil-fired power plant, this  $EF$  is 762 gCO<sub>2</sub>eq/kWh [55]. Therefore, the impact of decarbonization in tons of CO<sub>2</sub>eq/kWh ( $E_{CO_2}$ ) can be determined using Equation (11) [55].

$$E_{CO_2} = EF \cdot P \cdot \text{hours} = 532 \cdot P \cdot 8760 \quad (11)$$

#### 2.4. Georeferenced Survey

The software QGIS 3.22 Białowieża<sup>®</sup> was used as a georeferencing tool to determine potential locations for wave energy generator farms. Initially, a survey of secondary data available in the literature and from government agencies such as (i) the Brazilian Institute of Geography and Statistics (IBGE), (ii) the Geological Survey of Brazil (CPRM), and (iii) the National Spatial Data Infrastructure (INDE) was conducted. These collected data were used as guidance for this study, supporting the verification of the prerequisites of a promontory area and steep slopes. In this study, georeferenced data in vector format for the territorial division of Brazilian states [84], a detailed profile of the Brazilian coast [85], ocean bathymetry with contour lines at 20 m intervals [85], geolocation of coral reefs and islands [86], and environmental conservation units [84] were required. The survey began at the southernmost point of the state of Rio Grande do Sul, at coordinate  $33^{\circ}44'38.4''$  S,  $53^{\circ}22'08.4''$  W, and extended to the northernmost point of the Brazilian coast, in the state of Amapá, at coordinate  $4^{\circ}27'03.6''$  N,  $51^{\circ}32'16.8''$  W. The coastline was surveyed at 1 km intervals along its entire length, identifying locations that met the conditions of being rocky outcrops (promontories) and having steeper slopes (above 0.01 m/m). These requirements are necessary to ensure that the structure has a sufficient amount of physical space for installation and has lower energy dissipation due to friction with the seabed. When a point was identified positively, its geographic coordinates were collected, followed by a calculation of the length of the location and the slope from the centroid of vector extension. The survey was used to produce a georeferenced shapefile and a data file (dataset) with suitable locations. Figure 5 shows a typical surveyed area that was determined to be compatible with the requirements of this study.

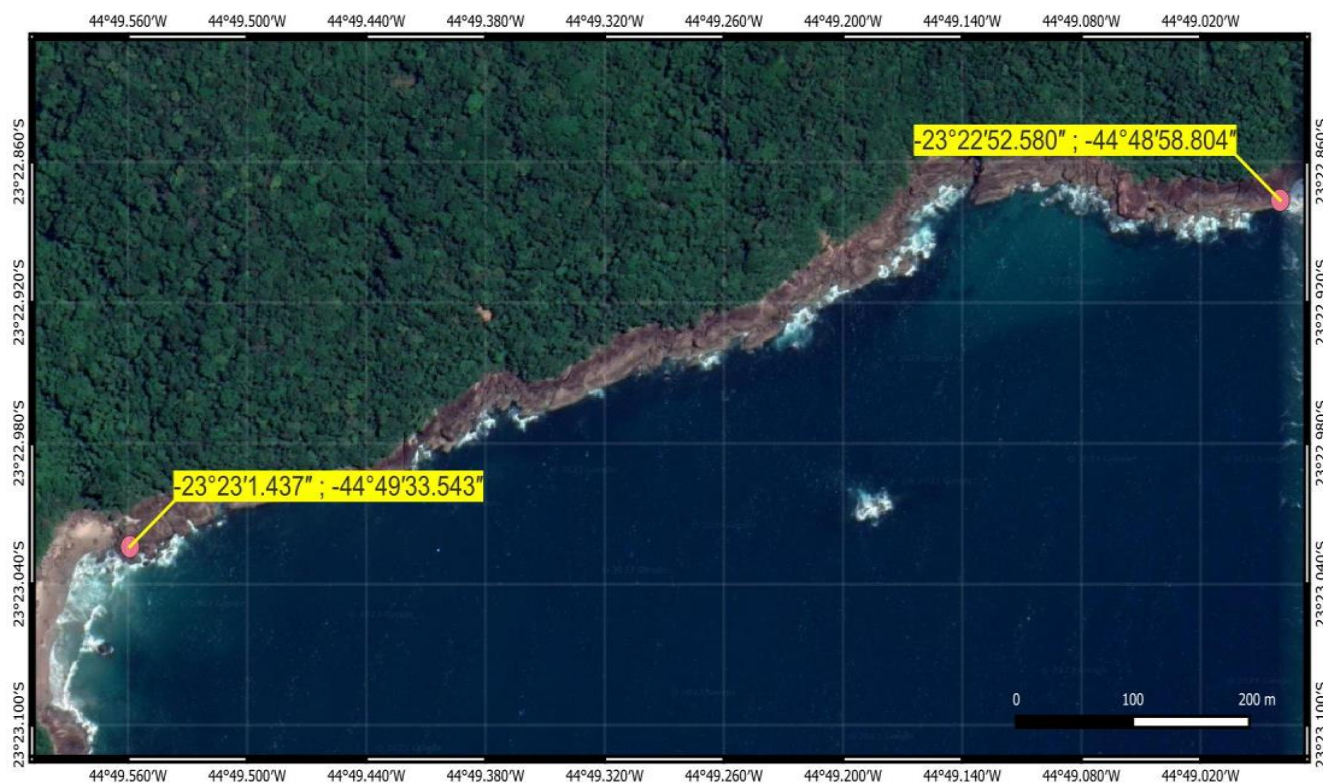


Figure 5. Representative point of a prospective location with rocky outcrops and steep slopes.

### 3. Results and Discussion

#### 3.1. Wave Climate and Energy Flux

Table 2 presents the significant wave height data ( $H_S P_{50}$ ;  $H_S P_{95}$ ;  $H_S MAX$ ) and peak wave period ( $T_e$ ) for the 49 distribution points along the Brazilian coast. Through these

values, it is possible to group the data corresponding to each coastal state. For states with extensive coastlines, we used the arithmetic average of the data in the grouping. In contrast, for states with smaller coastlines, we used values from a single distribution point. The data, the clusters, and their standards can be better observed in Table 2. However, Table 3 presents the results of  $\overline{H_S} P_{95} T_e$  that are used in this study and presents the result of the energy flux ( $E_f$ ) obtained through Equation (6), derived from Equations (1) to (5). The value shown already takes into account the 5% [70] energy loss from the spectral analysis point to the coastline due to flow friction with the seabed, shoaling, and refraction [70].

**Table 3.** Significant wave height, peak wave period, and energy flux values.

Coastal State	$\overline{H_S} P_{95}$ (m)	$T_e$ (s)	$E_f$ (kW/m)
Amapá	2.34	8.50	18.63
Pará	2.14	8.50	15.46
Maranhão	2.16	8.50	15.86
Piauí	2.18	8.00	15.17
Ceará	2.19	8.00	15.28
Rio Grande do Norte	2.20	8.00	15.45
Paraíba	2.28	8.00	16.60
Pernambuco	2.32	8.50	18.26
Alagoas	2.26	8.50	17.33
Sergipe	2.21	8.00	15.59
Bahia	2.20	8.00	15.47
Espírito Santo	2.40	9.00	20.65
Rio de Janeiro	2.68	9.50	27.18
São Paulo	2.69	9.50	27.37
Paraná	2.47	9.00	21.91
Santa Catarina	2.86	9.00	29.45
Rio Grande do Sul	3.28	9.00	38.59

As noted earlier (Section 2.1), the wave climate decays from south to north, directly impacting the potential for wave energy generation along the Brazilian coast [62,64,65].

### 3.2. Theoretical Potential of the Brazilian Coast

The theoretical potential of wave energy along the Brazilian coast can be estimated using the energy flux values ( $E_f$ ) from Table 3. The calculation was performed by multiplying the individual territorial extensions of each coastal state by its respective energy flux. Table 4 presents the results of each Brazilian state's potential theoretical capacity for coastal wave energy generation.

Table 4 shows a potential of nearly 70 GW of coastal wave energy throughout the Brazilian coast. This power reflects a generation capacity of 612.52 TWh/year, representing 98% of the national consumption in 2020 [3]. The northern region has 1177 km of coastlines and could contribute a wave energy capacity of 8.85 GW; the northeastern region has 3367 km and could contribute 23.46 GW. The southeast region, composed of Espírito Santo, Rio de Janeiro, and São Paulo, has 1675 km and could contribute 18.94 GW. The southern region has 1270 km and contributes 18.67 GW. As observed and already reported, there is an energy increase from north to south of the country, causing the south and southeast regions to represent 39% of the coastline and to be responsible for 54% of the estimated generation capacity.

**Table 4.** Theoretical potential of the Brazilian coast.

Region	Coastal State	Extension (km)	Flux (kW/m)	Power (GW)
North	Amapá	607	18.63	4.97
	Pará	570	15.46	3.88
Northeast	Maranhão	650	15.86	4.54
	Piauí	67	15.17	0.45
	Ceará	582	15.28	3.91
	Rio Grande do Norte	416	15.45	2.83
	Paraíba	119	16.60	0.87
	Pernambuco	190	18.26	1.53
	Alagoas	232	17.33	1.77
	Sergipe	165	15.59	1.13
	Bahia	946	15.47	6.44
Southeast	Espírito Santo	398	20.65	3.62
	Rio de Janeiro	646	27.18	7.73
	São Paulo	631	27.37	7.60
South	Paraná	99	21.91	0.95
	Santa Catarina	539	29.45	6.98
	Rio Grande do Sul	632	38.59	10.73
				69.92

### 3.3. Oscillating Water Column Wave Energy Potential

The georeferenced survey realized by the QGIS<sup>®</sup> identified 319 locations suitable for implementing coastal generator farms along the Brazilian coast. All these locations met the requirements of being rocky outcrops and having a slope greater than 0.01 m/m, which makes them suitable for receiving shoreline generator devices. However, only ten in seventeen coastal states have such locations suitable for implementing generator farms. Table 5 presents the values resulting from the georeferenced prospect, including the energetic calculation values for the states that showed potential for the implementation of coastal wave energy farms: (i) the number of locations capable of supporting wave energy farms under the conditions of this study, (ii) the individual extensions prospected for each state, (iii) the available energy flux values, (iv) the possible installed power, and (v) the available energy. A detailed description of the energy inventory points and their geographic coordinates is available in Annex S1 as Supplementary Materials.

**Table 5.** Oscillating water column potential resulting from the georeferenced survey.

	Coastal State	Farms	Extension (km)	Flux (kW/m)	Power (MW)	Energy (GWh)
Northeast	Ceará	6	5.65	15.28	37.97	332.64
	Rio Grande do Norte	3	1.86	15.45	12.64	110.74
	Pernambuco	6	10.92	18.26	87.71	768.35
	Bahia	13	14.64	15.47	99.65	872.95
Southeast	Espírito Santo	21	29.90	20.65	271.61	2379.31
	Rio de Janeiro	88	256.13	27.18	3063.07	26,832.49
	São Paulo	94	337.28	27.37	4061.18	35,575.94
South	Paraná	3	1.32	21.91	12.73	111.52
	Santa Catarina	82	139.46	29.45	1806.99	15,829.27
	Rio Grande do Sul	3	5.89	38.59	100.07	876.60
					9553.63	83,689.81

The coastal regions of Ceará, Rio Grande do Norte, Pernambuco, Bahia, Espírito Santo, Paraná, and Rio Grande do Sul also have predominantly sandy and low-slope areas,

except for some promontories. The Rio de Janeiro, São Paulo, and Santa Catarina states are characterized by large rocky outcrops.

The OWCMs included in this study, described in Section 2.3, and calculated by Equation (7), have a hydropneumatic chamber opening of 6 m in width, with power ratings of 55 kW, 75 kW, and 100 kW (which correspond to increasing energy flow from the north to south of the Brazilian coast). The total power obtained from these standardized modules represents a capacity that is 3% higher than initially calculated. However, in some states, standardization may result in power increases from 14% up to 36%, as is the case in the states of Ceará (36%), Rio Grande do Norte (34%), Pernambuco (14%), Bahia (34%), and Paraná (28%). In other states, this increase varies from 1% in Espírito Santo to 4% in Rio de Janeiro and São Paulo. For the states of Santa Catarina and Rio Grande do Sul, standardization results in a reduction in the capacity by 4% and 2%, respectively. This decrease results in a reduction in available energy in the states of Santa Catarina and Rio Grande do Sul, which, when compared to the sum of all the states, represents a decrease of 0.7% in the available energy for these states on the Brazilian coast, which can be considered negligible at this level of study. It is estimated that, instead of being a cost-increasing element, standardized production of these modules could lead to lower installation costs. Table 6 summarizes the values obtained for the survey of locations using the proposed OWCMs.

**Table 6.** Oscillating water column micro-module potential resulting from the georeferenced survey.

	Coastal State	Number of OWCM	Flux (kW/m)	Power (MW)	Energy (GWh)
Northeast	Ceará	939	15.28	51.65	332.64
	Rio Grande do Norte	308	15.45	16.94	110.74
	Pernambuco	1816	18.26	99.88	768.35
	Bahia	2434	15.47	133.87	872.95
Southeast	Espírito Santo	4970	20.65	273.35	2379.31
	Rio de Janeiro	42,646	27.18	3198.45	26,832.49
	São Paulo	56,162	27.37	4212.15	35,575.94
South	Paraná	218	21.91	16.35	111.52
	Santa Catarina	23,205	29.45	1740.38	15,245.77
	Rio Grande do Sul	980	38.59	98.00	858.50
				9841.01	83,088.21

Figure 6 graphically presents the energy results obtained by the georeferenced survey, demonstrating that the southeast region is responsible for 77% of the potential identified, with Espírito Santo having 273 MW, Rio de Janeiro having 3063 MW, and São Paulo having 4061 MW.

The georeferenced survey results showed that there is a potential of almost 10 GW of wave energy to be exploited. The value corresponds to 11.5% of the estimated 87 GW wave energy potential in the literature [9]. Brazil's southeast region is the most populous and industrialized, with 89.01 million inhabitants (over 40% of the country's total population) and responsible for over 55% of the national GDP. In 2020, the region consumed 303 TWh, corresponding to 49% of the energy system. Implementing almost 9.84 GW of wave energy, which represents 5% of the total installed capacity in Brazil, could supply 27% of the southeast's energy consumption, considering that its geographical location is strategically well within the region, which implies a decrease in transmission losses.

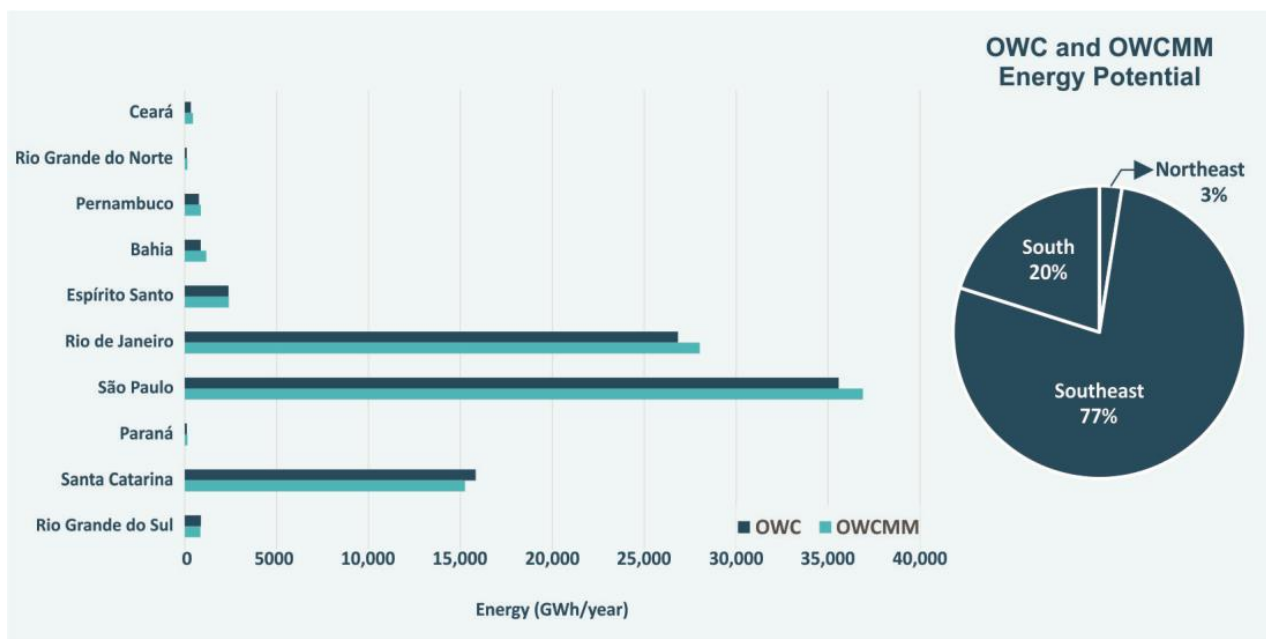


Figure 6. Oscillating water column wave energy potential. Source: Author.

### 3.4. Economic Evaluation

To conduct the economic evaluation of the OWCMM, the following assumptions were made: (i) the unit costs of the modules can range between 3000 and 14,000 USD/kW installed; (ii) the payback can range between 4 and 12 years, which covers the range recommended by Callaghan (2006) [30]; and (iii) the interest rate will be 12% per year. Table 7 presents the annual capital cost, O&M cost, and the cost of generated energy for each kW installed under the above assumptions and calculated from Equations (8) to (11). The calculations were performed in a unitary manner so that they can be used for the three proposed classes of modules (55, 75, and 100 kW). Figure 7 shows a graph that illustrates the possible values of the cost of energy generation as a function of the expected payback and the unit cost (USD/kW).

Table 7. Annual capital cost, O&M cost, and cost of energy generated per installed kW.

Unit Cost (USD/kW)	Annual Cost (Capital + O&M Cost)					Cost of Generated Energy				
	Payback					Payback				
	4 Years	6 Years	8 Years	10 Years	12 Years	4 Years	6 Years	8 Years	10 Years	12 Years
3000	1137.70	879.68	753.91	680.95	634.31	0.144	0.112	0.096	0.086	0.080
4000	1516.94	1172.90	1005.21	907.94	845.75	0.192	0.149	0.128	0.115	0.107
5000	1896.17	1466.13	1256.51	1134.92	1057.18	0.241	0.186	0.159	0.144	0.134
6000	2275.41	1759.35	1507.82	1361.90	1268.62	0.289	0.223	0.191	0.173	0.161
7000	2654.64	2052.58	1759.12	1588.89	1480.06	0.337	0.260	0.223	0.202	0.188
8000	3033.88	2345.81	2010.42	1815.87	1691.49	0.385	0.298	0.255	0.230	0.215
9000	3413.11	2639.03	2261.73	2042.86	1902.93	0.433	0.335	0.287	0.259	0.241
10,000	3792.34	2932.26	2513.03	2269.84	2114.37	0.481	0.372	0.319	0.288	0.268
11,000	4171.58	3225.48	2764.33	2496.83	2325.80	0.529	0.409	0.351	0.317	0.295
12,000	4550.81	3518.71	3015.63	2723.81	2537.24	0.577	0.446	0.383	0.345	0.322
13,000	4930.05	3811.93	3266.94	2950.79	2748.68	0.625	0.484	0.414	0.374	0.349
14,000	5309.28	4105.16	3518.24	3177.78	2960.12	0.673	0.521	0.446	0.403	0.375

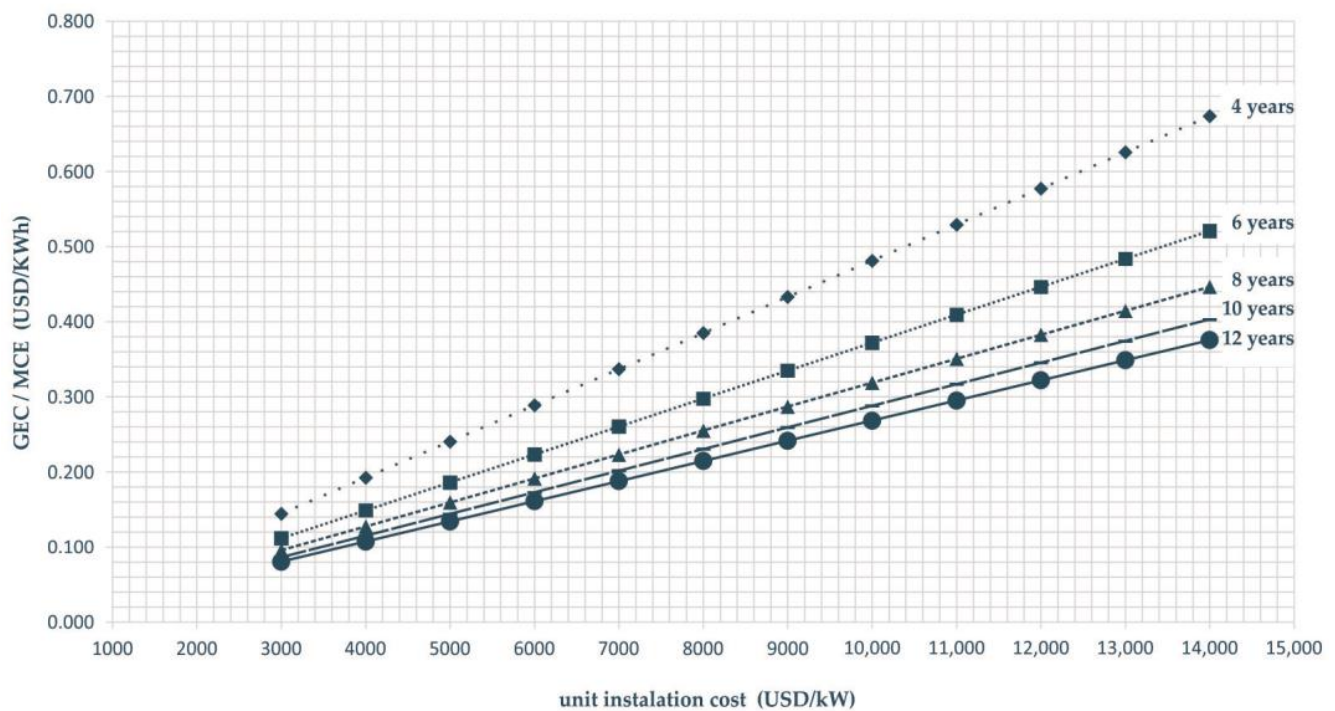


**Figure 7.** Payback analyses. Source: Author.

This graph allows us to investigate the maximum value that the installation can have in relation to market energy cost, based on an expected return time.

As indicated in Figure 7, if the installation has a unit cost of 7000 USD/kW and a payback of 12 years, the value of the generated energy will be 0.197 USD/kWh. If the assumed payback were 4 years, the value of the generated energy would be 0.340 USD/kWh. Similarly, if the market cost of energy (MCE) were 0.400 USD/kWh, the installation could have a unit cost of 8000 USD/kW for a payback of 4 years and 14,000 USD/kW for a payback of 10 years. According to data from the Brazilian Government [87], the cost of purchasing energy through an auction was 54.78 USD/kWh in May 2022.

### 3.5. Oscillating Water Column Harvesting Georeferenced Map

All 319 surveyed locations were used for a shapefile map with a dataset of values, including (i) the Federative State to the location, (ii) geographic coordinates, (iii) the length of the stretch viable for implementing farms, (iv) the number of OWC micro-modules, (v) the potential and the energy for OWC device, and (vi) the potential and energy for the OWC micro-module. Figure 8 shows a representative view of the many possible representations that could be generated from the map resulting from this study. The figure shows the state of Ceará and its six prospective farms.

This georeferenced map has diverse uses. It can be grouped and broken into different views, providing information on the potential for coastal ocean energy exploration through OWC devices.

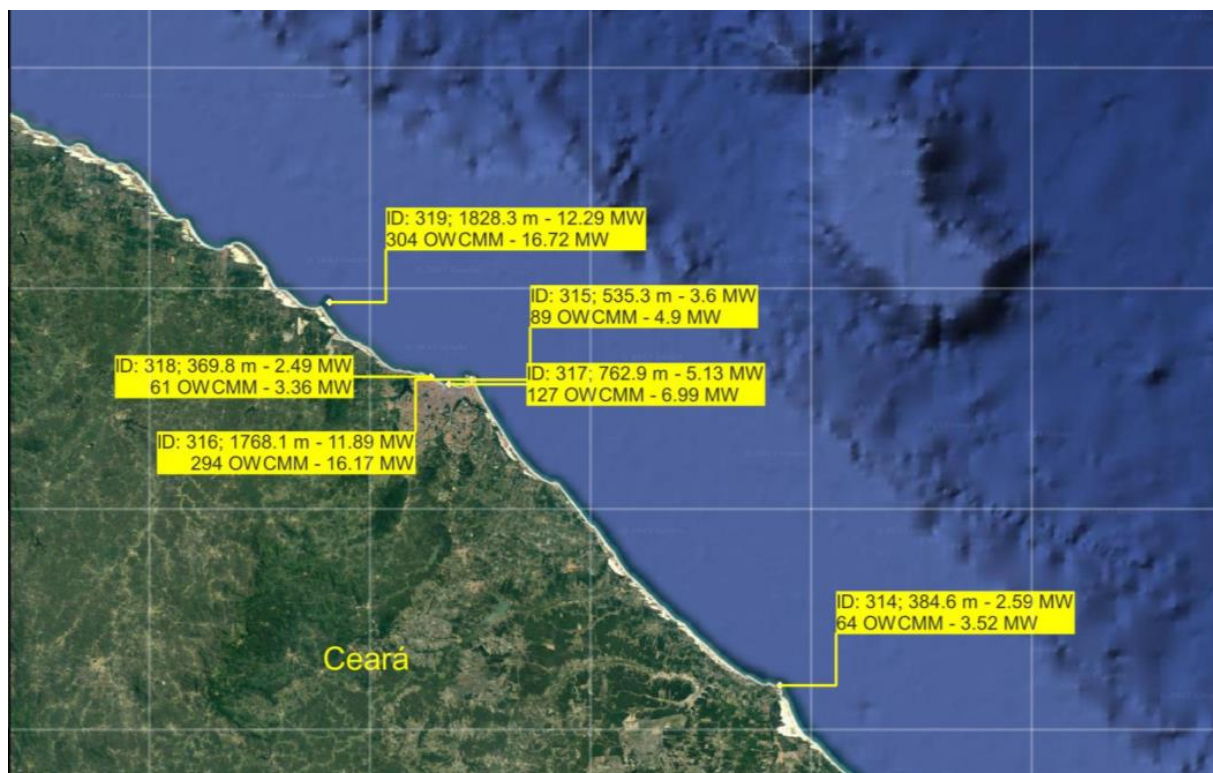


**Figure 8.** Georeferenced inventory in Ceará state module type 1–55 kW.

### 3.6. Zero Carbon Analyses

To determine the potential reduction in CO<sub>2</sub>eq emissions, assuming the implementation of wave energy generation on the Brazilian coast, Equation (10) was used. This energy substitution resulted in a total of 44.52 million t CO<sub>2</sub>eq emissions avoided per year for natural gas power plants, presented in Table 8. However, when applying this equation to oil-fired power plants, the value reaches 63.77 million tCO<sub>2</sub>eq per year. By considering only the potential of the southeast region, it would be possible to avoid emitting 34.46 MtCO<sub>2</sub>eq, contributing to the national decarbonization goals [1,6].

**Table 8.** Zero carbon results.

	Coastal State	Energy (GWh)	Emissions tonCO <sub>2</sub> eq
Northeast	Ceará	332.64	176,964
	Rio Grande do Norte	110.74	58,914
	Pernambuco	768.35	408,762
	Bahia	872.95	464,409
Southeast	Espírito Santo	2379.31	1,265,793
	Rio de Janeiro	26,832.49	14,274,885
	São Paulo	35,575.94	18,926,400
South	Paraná	111.52	59,329
	Santa Catarina	15,829.27	8,421,172
	Rio Grande do Sul	876.60	466,351
			44,522,979

## 4. Conclusions

Technological challenges, current implementation costs, and converter device efficiency are limiting factors for the immediate adoption of wave energy resources in Brazil.

Nonetheless, wave energy generation is advantageous as it is a clean and renewable energy source, in line with the decarbonization goals proposed in Brazil's NDC. This study concludes that there is an easily accessible exploitable potential of 9.84 GW (already considering an efficiency of 44%) for coastal OWC, which would represent a maximum annual energy availability of 83 TWh/year. This amount of energy is virtually equivalent to the energy consumption of the entire northeast region in 2020 (81 TWh), and replacing the thermal gas energy consumed in this region with wave energy could potentially reduce around 44.52 million tons of CO<sub>2</sub>eq per year (10% of national emissions). The majority of this potential is located on the coast of three important states: São Paulo, Rio de Janeiro, and Santa Catarina, representing more than 94% of the generation capacity accounted for in this study. Together, these states cover more than 34% of the Brazilian population and are responsible for over 46% of the GDP. The economic analysis shows that the use of an OWCMM becomes viable at a market cost of energy (MCE) of 0.100 USD/kWh, with unit installation costs of 3000 USD/kW and a payback period of 12 years. If the payback period is reduced to 4 years, the MCE increases to 0.197 USD/kWh. With an installation cost of 12,000 USD/kW, the GEC ranges from 0.300 to 0.540 USD/kWh. Comparing this value with energy auction prices in Brazil, it can be seen that, at best, it is still twice as high as current market prices. Although 84% of the Brazilian energy matrix comes from renewable sources, it could still benefit from the generation capacity of OWCMM, which represents 10% of the hydroelectric generation capacity, but could replace 100% of oil-based generation. This highlights that the introduction of wave energy in Brazil will require government incentives, such as tax reductions and subsidies for the installation of generating parks. Finally, this result suggests that wave energy generation can be included in future expansion studies of the Brazilian power system as an accelerating factor in the energy transition, to the detriment of new carbon-based generation projects, as outlined in the PNE 2050. It is suggested to continue studies on ocean potentials on the Brazilian coast, evaluating the potential of other forms of wave energy conversion and other forms of ocean energy, such as ocean thermal energy, highlighted as promising in Brazil's PNE 2050. The continuation of this study is also recommended, analyzing the efficiency and effectiveness of OWC micromodules through a reduced physical model, as well as expanding upon studies on the environmental impacts caused by the installation of large generator parks equipped with OWCMM devices.

**Supplementary Materials:** The following supporting information can be downloaded at: <https://www.mdpi.com/article/10.3390/en16083409/s1>, Table S1: Georeferenced inventory summary.

**Author Contributions:** Conceptualization, A.S.B. and C.B.M.; methodology, A.S.B. and C.B.M.; software, A.S.B.; validation, A.S.B., M.d.L.N.M.M. and C.B.M.; formal analysis, A.S.B., M.d.L.N.M.M.; investigation, A.S.B., D.S.R. and C.B.M.; resources, A.S.B. and C.B.M.; data curation, A.S.B. and T.R.C.d.S.; writing—original draft preparation, A.S.B., T.R.C.d.S., D.S.R., M.d.L.N.M.M. and C.B.M.; writing—review and editing, A.S.B., T.R.C.d.S., D.S.R., M.d.L.N.M.M. and C.B.M.; visualization, A.S.B., T.R.C.d.S., D.S.R., M.d.L.N.M.M. and C.B.M.; funding acquisition, C.B.M. All authors have read and agreed to the published version of the manuscript.

**Funding:** This research was funded by Coordenação de Aperfeiçoamento de Pessoal de Nível Superior—Brasil (CAPES)—Finance Code 001; CNPq—license number PQ: 304370/2018-5/305059/2022-0; Fapemig—license number PPM-00252-18; award of doctorate level scholarship—process number 88882.381136/2019-01; and SEFAC/ANEEL—license number PD-06899-2912/2016 & PD-06899-2812/2016.

**Data Availability Statement:** The data presented in this study are available in article or Supplementary Material.

**Acknowledgments:** This study was financed in part by the Coordenação de Aperfeiçoamento de Pessoal de Nível Superior—Brasil (CAPES)—Finance Code 001.

**Conflicts of Interest:** The authors declare no conflict of interest.

## Abbreviations

CPRM	Geological Survey of Brazil
GHG	Greenhouse gas
IBGE	Brazilian Institute of Geography and Statistics
INDE	National Spatial Data Infrastructure
IRENA	International Renewable Energy Agency
NDC	Nationally Determined Contribution
OWC	Oscillating water column
OWCMM	OWC micro-modules
PNE	Brazil's National Energy Plan
PRO	Pressure Retarded Osmosis
RED	Reverse Electrodialysis
SDG	Sustainable Development Goals
UN	United Nations
UNDP	United Nations Development Program
USD	American dollar

## Nomenclature

$C$	Wave celerity	GW	Gigawatt
$C_g$	Group velocity	GWh	Gigawatt-hours
$D_s$	Wave direction	kW	Kilowatt
$EF$	Emission factor	kWh	Kilowatt-hours
$E_f$	Energy flux	m/s	Meters per second
$E_K$	Kinetic energy	MW	Megawatt
$EP$	Potential energy	MWh	Megawatt hours
$\omega$	Angular frequency	N/m <sup>2</sup>	Newtons per square meter
$h$	Local depth	TW	Terawatt
$H$	Individual wave height	TWh	Terawatt-hours
$H_s$	Significant wave height	W	Watt
$k$	Wave number	W/m	Watt per meter
$L$	Wavelength		
$n$	Wave celerity factor	CO <sub>2</sub>	Carbon dioxide
$T_e$	Peak wave period	tCO <sub>2</sub> eq	Tons of CO <sub>2</sub> equivalent
$\rho$	Seawater density		
$\omega$	Angular frequency		

## References

1. UNDP Sustainable Development Goals. Available online: <https://www.undp.org/sustainable-development-goals> (accessed on 10 March 2022).
2. Smil, V. *Energy Transitions: History, Requirements, Prospects*, 1st ed.; ABC-CLIO: Santa Barbara, CA, USA, 2010; Volume 1, ISBN 978-0-313-38177-5.
3. EPE, Empresa de Pesquisa Energética. *2021 Statistical Yearbook of Electricity—2020 Baseline Year*; MME: Brasília, Brazil, 2021.
4. European Union. EDGAR—The Emissions Database for Global Atmospheric Research. Available online: [https://edgar.jrc.ec.europa.eu/report\\_2022](https://edgar.jrc.ec.europa.eu/report_2022) (accessed on 31 March 2023).
5. Falkner, R. The Paris Agreement and the New Logic of International Climate Politics. *Int. Aff.* **2016**, *92*, 1107–1125. [CrossRef]
6. UNFCCC Nationally Determined Contributions Registry. Available online: [https://unfccc.int/NDCREG?gclid=Cj0KCQiA6rCgBhDVARIsAK1kGPIsCgQYxjBQBWEjC2y0E7MJKI7J8iOrmGn4xXPadLadDpNwmnxVgaAiyBEALw\\_wcB](https://unfccc.int/NDCREG?gclid=Cj0KCQiA6rCgBhDVARIsAK1kGPIsCgQYxjBQBWEjC2y0E7MJKI7J8iOrmGn4xXPadLadDpNwmnxVgaAiyBEALw_wcB) (accessed on 10 March 2022).
7. MME. *National Energy Plan—PNE 2030*; MME: Rio de Janeiro, Brazil, 2006. Available online: <https://www.epe.gov.br/sites-pt/publicacoes-dados-abertos/publicacoes/Documents/Relat%c3%b3rio%20final%20PNE%202030.pdf> (accessed on 10 April 2023).
8. MME. *National Energy Plan—PNE 2050*; MME: Rio de Janeiro, Brazil, 2020. Available online: <https://www.epe.gov.br/sites-pt/publicacoes-dados-abertos/publicacoes/PublicacoesArquivos/publicacao-227/topico-563/Relatorio%20Final%20do%20PNE%202050.pdf> (accessed on 10 April 2023).
9. Tolmasquim, M.T. *Energia Renovável: Hidráulica, Biomassa, Eólica, Solar, Oceânica*, 1st ed.; EPE, Empresa de Pesquisa Energética: Rio de Janeiro, Brazil, 2016; Volume 1, ISBN 978-85-60025-06-0.

10. Bezerra Leite Neto, P.; Ronald Saavedra, O.; Camelo, N.J.; de Souza Ribeiro, L.A.; Ferreira, R.M. Exploração de Energia Maremotriz Para Geração de Eletricidade: Aspectos Básicos e Principais Tendências. *Ingeniare Rev. Chil. Ing.* **2011**, *19*, 219–232. [[CrossRef](#)]
11. Estefen, S.F.; Garcia-Rosa, P.B.; Ricarte, E.; da Costa, P.R.; Pinheiro, M.M.; Lourenço, M.I.; Machado, I.R.; Maes, S.R. Wave Energy Hyperbaric Converter: Small Scale Models, Prototype and Control Strategies. Proceedings of International Conference on Ocean, Offshore, and Arctic Engineering (OMAE), Rio de Janeiro, Brazil, 1–6 July 2012; pp. 649–657.
12. Shadman, M.; Silva, C.; Faller, D.; Wu, Z.; de Freitas Assad, L.; Landau, L.; Levi, C.; Estefen, S. Ocean Renewable Energy Potential, Technology, and Deployments: A Case Study of Brazil. *Energies* **2019**, *12*, 3658. [[CrossRef](#)]
13. Falcão, A.F.O. Wave Energy Utilization: A Review of the Technologies. *Renew. Sustain. Energy Rev.* **2010**, *14*, 899–918. [[CrossRef](#)]
14. Falnes, J. A Review of Wave-Energy Extraction. *Mar. Struct.* **2007**, *20*, 185–201. [[CrossRef](#)]
15. Falcão, A.F.O.; Henriques, J.C.C. Oscillating-Water-Column Wave Energy Converters and Air Turbines: A Review. *Renew. Energy* **2016**, *85*, 1391–1424. [[CrossRef](#)]
16. Salter, S.H. Wave Power. *Nature* **1974**, *249*, 720–724. [[CrossRef](#)]
17. McCormick, M.E. *Ocean Wave Energy Conversion*; Wiley-Interscience: Hoboken, NJ, USA, 1981.
18. Evans, D.V. A Theory for Wave-Power Absorption by Oscillating Bodies. *J. Fluid Mech.* **1976**, *77*, 1–25. [[CrossRef](#)]
19. Evans, D.V.; Porter, R. Efficient Calculation of Hydrodynamic Properties of OWC-Type Devices. *J. Offshore Mech. Arct. Eng.* **1997**, *119*, 210–218. [[CrossRef](#)]
20. Falnes, J.; McIver, P. Surface Wave Interactions with Systems of Oscillating Bodies and Pressure Distributions. *Appl. Ocean. Res.* **1985**, *7*, 225–234. [[CrossRef](#)]
21. Falcão, A.F.O.; Sarmiento, A.J.N.A.; Gato, L.M.C.; Brito-Melo, A. The Pico OWC Wave Power Plant: Its Lifetime from Conception to Closure 1986–2018. *Appl. Ocean. Res.* **2020**, *98*, 102104. [[CrossRef](#)]
22. Falcão, A.F.O. First-Generation Wave Power Plants: Current Status and RD Requirements. In Proceedings of the International Conference on Ocean, Offshore, and Arctic Engineering (OMAE), Cancun, Mexico, 8–13 January 2003.
23. Falcão, A.F.O.; Gato, L.M.C.; Nunes, E.P.A.S. A Novel Radial Self-Rectifying Air Turbine for Use in Wave Energy Converters. *Renew. Energy* **2013**, *50*, 289–298. [[CrossRef](#)]
24. Gato, L.M.C.; Falcão, A.F.O. Aerodynamics of the Wells Turbine. *Int. J. Mech. Sci.* **1988**, *30*, 383–395. [[CrossRef](#)]
25. Gato, L.M.C.; Falcão, A.F. On the Theory of the Wells Turbine. *J. Eng. Gas Turbines Power* **1984**, *106*, 628–633. [[CrossRef](#)]
26. Setoguchi, T.; Santhakumar, S.; Takao, M.; Kim, T.H.; Kaneko, K. A Modified Wells Turbine for Wave Energy Conversion. *Renew. Energy* **2003**, *28*, 79–91. [[CrossRef](#)]
27. Setoguchi, T.; Kim, T.W.; Takao, M.; Thakker, A.; Raghunathan, S. The Effect of Rotor Geometry on the Performance of a Wells Turbine for Wave Energy Conversion. *Int. J. Ambient. Energy* **2004**, *25*, 137–150. [[CrossRef](#)]
28. Raghunathan, S. The Wells Air Turbine for Wave Energy Conversion. *Prog. Aerosp. Sci.* **1995**, *31*, 335–386. [[CrossRef](#)]
29. Raghunathan, S.; Tan, C.P. Aerodynamic Performance of a Wells Air Turbine. *J. Energy* **1983**, *7*, 226–230. [[CrossRef](#)]
30. Callaghan, J. Future Marine Energy. Results of the Marine Energy Challenge: Cost Competitiveness and Growth of Wave and Tidal Stream Energy. 2006. Available online: <http://large.stanford.edu/courses/2012/ph240/thomas2/docs/futuremarineenergy.pdf> (accessed on 3 April 2023).
31. Zabihian, F.; Fung, A.S. Review of Marine Renewable Energies: Case Study of Iran. *Renew. Sustain. Energy Rev.* **2011**, *15*, 2461–2474. [[CrossRef](#)]
32. Khan, M.Z.A.; Khan, H.A.; Aziz, M. Harvesting Energy from Ocean: Technologies and Perspectives. *Energies* **2022**, *15*, 3456. [[CrossRef](#)]
33. Post, J.W.; Veerman, J.; Hamelers, H.V.M.; Euverink, G.J.W.; Metz, S.J.; Nymeyer, K.; Buisman, C.J.N. Salinity-Gradient Power: Evaluation of Pressure-Retarded Osmosis and Reverse Electrodialysis. *J. Membr. Sci.* **2007**, *288*, 218–230. [[CrossRef](#)]
34. Zhang, W.; Li, Y.; Wu, X.; Guo, S. Review of the Applied Mechanical Problems in Ocean Thermal Energy Conversion. *Renew. Sustain. Energy Rev.* **2018**, *93*, 231–244. [[CrossRef](#)]
35. Hussain, A.; Arif, S.M.; Aslam, M. Emerging Renewable and Sustainable Energy Technologies: State of the Art. *Renew. Sustain. Energy Rev.* **2017**, *71*, 12–28. [[CrossRef](#)]
36. Neill, S.P.; Angeloudis, A.; Robins, P.E.; Walkington, I.; Ward, S.L.; Masters, I.; Lewis, M.J.; Piano, M.; Avdis, A.; Piggott, M.D.; et al. Tidal Range Energy Resource and Optimization—Past Perspectives and Future Challenges. *Renew. Energy* **2018**, *127*, 763–778. [[CrossRef](#)]
37. Khaligh, A.; Onar, O.C. Ocean Wave Energy Harvesting. In *Energy Harvesting: Solar, Wind, and Ocean Energy Conversion Systems*; CRC Press: Boca Raton, FL, USA, 2010; pp. 223–303. ISBN 978-1-4398-1508-3.
38. Barbarelli, S.; Nastasi, B. Tides and Tidal Currents—Guidelines for Site and Energy Resource Assessment. *Energies* **2021**, *14*, 6123. [[CrossRef](#)]
39. de Andres, A.; Medina-Lopez, E.; Crooks, D.; Roberts, O.; Jeffrey, H. On the Reversed LCOE Calculation: Design Constraints for Wave Energy Commercialization. *Int. J. Mar. Energy* **2017**, *18*, 88–108. [[CrossRef](#)]
40. Contestabile, P.; Crispino, G.; Di Lauro, E.; Ferrante, V.; Gisonni, C.; Vicinanza, D. Overtopping Breakwater for Wave Energy Conversion: Review of State of Art, Recent Advancements and What Lies Ahead. *Renew. Energy* **2020**, *147*, 705–718. [[CrossRef](#)]
41. Knight, C.; McGarry, S.; Hayward, J.; Osman, P.; Behrens, S. A Review of Ocean Energy Converters, with an Australian Focus. *AIMS Energy* **2014**, *2*, 295–320. [[CrossRef](#)]

42. Drew, B.; Plummer, A.R.; Sahinkaya, M.N. A Review of Wave Energy Converter Technology. *Proc. Inst. Mech. Eng. Part A J. Power Energy* **2009**, *223*, 887–902. [CrossRef]
43. Henderson, R. Design, Simulation, and Testing of a Novel Hydraulic Power Take-off System for the Pelamis Wave Energy Converter. *Renew. Energy* **2006**, *31*, 271–283. [CrossRef]
44. Aderinto, T.; Li, H. Ocean Wave Energy Converters: Status and Challenges. *Energies* **2018**, *11*, 1250. [CrossRef]
45. Faizal, M.; Ahmed, M.R.; Lee, Y.-H. A Design Outline for Floating Point Absorber Wave Energy Converters. *Adv. Mech. Eng.* **2014**, *6*, 846097. [CrossRef]
46. Aderinto, T.; Li, H. Review on Power Performance and Efficiency of Wave Energy Converters. *Energies* **2019**, *12*, 4329. [CrossRef]
47. Lin, Y.; Bao, J.; Liu, H.; Li, W.; Tu, L.; Zhang, D. Review of Hydraulic Transmission Technologies for Wave Power Generation. *Renew. Sustain. Energy Rev.* **2015**, *50*, 194–203. [CrossRef]
48. IRENA. *Innovation Outlook: Ocean Energy Technologies*; IRENA: Abu Dhabi, United Arab Emirates, 2020.
49. IRENA. *Renewable Capacity Statistics 2020*; IRENA: Abu Dhabi, United Arab Emirates, 2020.
50. OES. OES | Ocean Energy Systems. Available online: <https://www.ocean-energy-systems.org/> (accessed on 17 April 2021).
51. Lekube, J.; Garrido, A.J.; Garrido, I.; Otaola, E. Output Power Improvement in Oscillating Water Column-Based Wave Power Plants. *Rev. Iberoam. Autom. E Inf. Ind.* **2018**, *15*, 145. [CrossRef]
52. Rosati, M.; Henriques, J.C.C.; Ringwood, J.V. Oscillating-Water-Column Wave Energy Converters: A Critical Review of Numerical Modelling and Control. *Energy Convers. Manag. X* **2022**, *16*, 100322. [CrossRef]
53. Ilyas, A.; Kashif, S.A.R.; Saqib, M.A.; Asad, M.M. Wave Electrical Energy Systems: Implementation, Challenges and Environmental Issues. *Renew. Sustain. Energy Rev.* **2014**, *40*, 260–268. [CrossRef]
54. Edenhofer, O.; Madrugá, R.P.; Sokona, Y.; Seyboth, K.; Eickemeier, P.; Matschoss, P.; Hansen, G.; Kadner, S.; Schlömer, S.; Zwickel, T.; et al. *Renewable Energy Sources and Climate Change Mitigation—Special Report of the Intergovernmental Panel on Climate Change*, 1st ed.; Cambridge University Press: New York, NY, USA, 2012; ISBN 978-1-107-60710-1.
55. IPCC. *IPCC AR6 Climate Change 2021: The Physical Science Basis*; Cambridge University Press: Cambridge, UK, 2021.
56. Zhang, Y.; Zhao, Y.; Sun, W.; Li, J. Ocean Wave Energy Converters: Technical Principle, Device Realization, and Performance Evaluation. *Renew. Sustain. Energy Rev.* **2021**, *141*, 110764. [CrossRef]
57. Raghunathan, S.; Tan, C.P. Performance of the Wells Turbine at Starting. *J. Energy* **1982**, *6*, 430–431. [CrossRef]
58. Curto, D.; Franzitta, V.; Guercio, A. Sea Wave Energy. A Review of the Current Technologies and Perspectives. *Energies* **2021**, *14*, 6604. [CrossRef]
59. Castro-Santos, L.; Silva, D.; Bento, A.; Salvação, N.; Guedes Soares, C. Economic Feasibility of Wave Energy Farms in Portugal. *Energies* **2018**, *11*, 3149. [CrossRef]
60. Holthuijsen, H. *Waves in Oceanic and Coastal Waters*; Cambridge University Press: Cambridge, UK, 2007.
61. Dean, R.G.; Dalrymple, R.A. *Water Wave Mechanics for Engineers and Scientists*, 1st ed.; World Scientific Publishing Co.: Hackensack, NJ, USA, 1991; ISBN 9810204205.
62. Pianca, C.; Mazzini, P.L.F.; Siegle, E. Brazilian Offshore Wave Climate Based on NWW3 Reanalysis. *Braz. J. Oceanogr.* **2010**, *58*, 53–70. [CrossRef]
63. Tolman, H.L. *User Manual and System Documentation of WAVEWATCH III TM Version 4.18*; NOAA: Washington, DC, USA, 2014.
64. Carvalho, J.T. *Simulação da Distribuição de Energia das Ondas Oceânicas Ao Largo do Litoral Brasileiro*; Instituto Nacional de Pesquisas Espaciais (INPE): São Paulo, Brazil, 2010.
65. Espindola, R.L. *Mapeamento de Sites Com Potencial para Geração de Energia Ondomotriz Por Meio de Análise de Decisão Multicritério*; Universidade Federal de Pernambuco: Recife, Brazil, 2017.
66. ECMWF ERA-Interim. Available online: <https://www.ecmwf.int/en/forecasts/datasets/reanalysis-datasets/era-interim> (accessed on 9 March 2020).
67. Cornett, A.M. A Global Wave Energy Resource Assessment. In Proceedings of the The Eighteenth International Offshore and Polar Engineering Conference, Vancouver, BC, Canada; 2008.
68. Fleming, F.P. *Avaliação do Potencial de Energias Oceânicas No Brasil*; Universidade Federal do Rio de Janeiro: Rio de Janeiro, Brazil, 2012.
69. Folley, M. The Wave Energy Resource. In *Handbook of Ocean Wave Energy*; Springer: Cham, Switzerland, 2017; pp. 43–79.
70. Ostritz, F.F. *Estimativa do Potencial Energético Gerado Por Ondas Na Costa do Brasil Com Ênfase No Estado do Ceará, Dissertação (Mestrado em Engenharia Oceânica)—COPPE; UFRJ: Rio de Janeiro, Brasil, 2012.*
71. Shehata, A.S. Investigation and Improvement of Wells Turbine Performance, Fluid Analysis & 2nd Law of Thermodynamics Study. Ph.D. Thesis, Universidade de Strathclyde, Glasgow, Scotland, 2016.
72. Lopes, B.S.C. *Construção e Ensaio de Um Modelo de Turbina de Ar Auto-Retificadora de Rotor Duplo para Sistemas de Aproveitamento da Energia das Ondas*; Universidade Técnica de Lisboa: Lisbon, Portugal, 2017.
73. Falcão, A.F.O.; Henriques, J.C.C.; Gato, L.M.C. Self-Rectifying Air Turbines for Wave Energy Conversion: A Comparative Analysis. *Renew. Sustain. Energy Rev.* **2018**, *91*, 1231–1241. [CrossRef]
74. Raghunathan, S.; Tan, C.; Ombaka, O. Performance of the Wells Self-Rectifying Air Turbine. *Aeronaut. J.* **1985**, *89*, 369–379. [CrossRef]
75. Mohamed, M.H.; Janiga, G.; Pap, E.; Thévenin, D. Multi-Objective Optimization of the Airfoil Shape of Wells Turbine Used for Wave Energy Conversion. *Energy* **2011**, *36*, 438–446. [CrossRef]

76. M'zoughi, F.; Garrido, I.; Garrido, A.J.; De La Sen, M. Rotational Speed Control Using ANN-Based MPPT for OWC Based on Surface Elevation Measurements. *Appl. Sci.* **2020**, *10*, 8975. [[CrossRef](#)]
77. Dizadji, N.; Sajadian, S.E. Modeling and Optimization of the Chamber of OWC System. *Energy* **2011**, *36*, 2360–2366. [[CrossRef](#)]
78. Ibarra-Berastegi, G.; Sáenz, J.; Ulazia, A.; Serras, P.; Esnaola, G.; Garcia-Soto, C. Electricity Production, Capacity Factor, and Plant Efficiency Index at the Mutriku Wave Farm (2014–2016). *Ocean. Eng.* **2018**, *147*, 20–29. [[CrossRef](#)]
79. Babarit, A. A Database of Capture Width Ratio of Wave Energy Converters. *Renew. Energy* **2015**, *80*, 610–628. [[CrossRef](#)]
80. Chen, J.; Wen, H.; Wang, Y.; Wang, G. A Correlation Study of Optimal Chamber Width with the Relative Front Wall Draught of Onshore OWC Device. *Energy* **2021**, *225*, 120307. [[CrossRef](#)]
81. Letzow, M.; Levien, F.V.; Pons, R.D.P.; Gomes, M.D.N.; Souza, J.A.; Rocha, L.A.O.; Isoldi, L.A.; Dos Santos, E.D. Avaliação Geométrica da Câmara de Um Dispositivo de Conversão de Energia das Ondas do Tipo OWC para Diferentes Comprimentos da Borda Frontal. *Rev. Bras. Energ. Renov.* **2017**, *6*, 454–471. [[CrossRef](#)]
82. Garrido, A.J.; Otaola, E.; Garrido, I.; Lekube, J.; Maseda, F.J.; Liria, P.; Mader, J. Mathematical Modeling of Oscillating Water Columns Wave-Structure Interaction in Ocean Energy Plants. *Math. Probl. Eng.* **2015**, *2015*, 727982. [[CrossRef](#)]
83. Bosserelle, C.; Reddy, S.; Krüger, J. *Waves and Coasts in the Pacific: Cost Analysis of Wave Energy in the Pacific*; Secretariat of the Pacific Community: Suva, Fiji, 2015.
84. IBGE. Portal de Mapas do IBGE. Available online: <https://portaldemapas.ibge.gov.br/portal.php#homepage> (accessed on 5 May 2021).
85. CPRM. GeoSGB. Available online: <http://geosgb.cprm.gov.br/> (accessed on 5 May 2021).
86. INDE. Portal INDE. Available online: <https://www.inde.gov.br/> (accessed on 5 May 2021).
87. Leilão de Energia Contrata 29 Empreendimentos Com Deságio de 9.36% | Agência Brasil. Available online: <https://agenciabrasil.ebc.com.br/economia/noticia/2022-05/leilao-de-energia-contrata-29-empreendimentos-com-desagio-de-936> (accessed on 3 April 2023).

**Disclaimer/Publisher's Note:** The statements, opinions and data contained in all publications are solely those of the individual author(s) and contributor(s) and not of MDPI and/or the editor(s). MDPI and/or the editor(s) disclaim responsibility for any injury to people or property resulting from any ideas, methods, instructions or products referred to in the content.